Journal of Rehabilitation in Civil Engineering 6-1 (2018) 132-147

journal homepage: http://civiljournal.semnan.ac.ir/

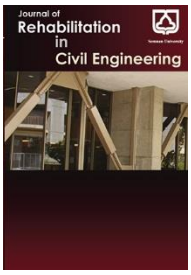

Modeling of Resilient Modulus of Asphalt Concrete Containing Reclaimed Asphalt Pavement Using Feed-Forward and Generalized Regression Neural Networks

A. Mansourian[1*], A.R. Ghanizadeh[2] and B. Golchin[3]

1. Department of Bitumen and Asphalt, Road, Housing and Urban Development Research Center, Tehran, Iran
2. Department of Civil Engineering, Sirjan University of Technology, Sirjan, Iran
3. Department of Civil Engineering, University of Mohaghegh Ardabili, Ardabil, Iran

Corresponding author: *email@semnan.ac.ir*

ARTICLE INFO

Article history:
Received: 16 March 2017
Accepted: 05 September 2017

Keywords:
Asphalt Pavement,
Reclaimed Asphalt,
Resilient Modulus,
Neural Networks.

ABSTRACT

Reclaimed asphalt pavement (RAP) is one of the waste materials that highway agencies promote to use in new construction or rehabilitation of highways pavement. Since the use of RAP can affect the resilient modulus and other structural properties of flexible pavement layers, this paper aims to employ two different artificial neural network (ANN) models for modeling and evaluating the effects of different percentages of RAP on resilient modulus of hot-mix asphalt (HMA). In this research, 216 resilient modulus tests were conducted for establishing the experimental dataset. Input variables for predicting resilient modulus were temperature, penetration grade of asphalt binder, loading frequency, change of asphalt binder content compared to optimum asphalt binder content and percentage of RAP. Results of modeling using feed-forward neural network (FFNN) and generalized regression neural network (GRNN) model were compared with the measured resilient modulus using two statistical indicators. Results showed that for FFNN model, the coefficient of determination between observed and predicted values of resilient modulus for training and testing sets were 0.993 and 0.981, respectively. These two values were 0.999 and 0.967 in case of GRNN. So, according to comparison of R2 for testing set, the accuracy of FFNN method was superior to GRNN method. Tests results and artificial neural network analysis showed that the temperature was the most effective parameter on the resilient modulus of HMA containing RAP materials. In addition by increasing RAP content, the resilient modulus of HMA increased.

DOI: 10.22075/JRCE.2017.10876.1177

1. Introduction

Each year large amount of asphalt concrete are produced from reclaimed asphalt pavement (RAP) [1]. Recently, highway departments promote the use of RAP in asphalt pavement rehabilitations. The use of RAP has effect on some basic properties of hot-mix asphalt (HMA) such as resilient modulus. Resilient modulus as a measure of the stiffness of asphalt concrete mixture is one of the fundamental parameters that is used in evaluating of materials quality and as an input for asphalt pavement design. Colbert and You [2] evaluated the hot-mix asphalt containing 15, 35, and 50% RAP experimentally and indicated that the RAP increased the resilient modulus by 52%. Sondag et al. [3] blended 0 to 50% RAP with virgin aggregates and recommended different percentages of RAP (10-50%) and the respective asphalt binder grades to yield the stiffness similar to a virgin mixture. Zaumanis and Mallick [4] investigated the approaches for increasing the amount of RAP in asphalt concrete mixtures and indicated that the stiffness of high content RAP asphalt concrete mixtures was higher than that of the virgin.

Nowadays, artificial neural network (ANN) technique has been widely applied in asphalt material studies. Tarefder et al. [5] used a four-layer feed-forward neural network to determine a mapping associating mix design and testing factors of asphalt concrete samples to predict their permeability. They observed an excellent agreement between simulation and laboratory data. Ozgan [6] applied an ANN based model for the results of Marshall stability tests. He concluded that experiment results and ANN model exhibit a good correlation. Xiao and Amirkhanian [7] used ANN approach for estimating stiffness behavior of rubberized asphalt concrete containing reclaimed asphalt pavement. Their results indicated that ANN techniques were more effective than traditional regression-based prediction models in predicting the fatigue life of the modified mixture. Zaghal [8] modeled creep compliance behavior of asphalt concretes using ANN technique. This study showed that the proposed model could effectively predict the creep compliance of asphalt concrete mixtures at different temperatures with different binders. ANN has been also used for prediction of resilient modules of asphalt concrete mixtures. They are shown in Table 1. Figure 1 shows the research framework.

This research focuses on the prediction of the resilient modulus of asphalt concrete mixtures containing different percentage of RAP. Two different ANN techniques including generalized regression neural network (GRNN) and feed-forward neural network (FFNN) were applied for prediction of resilient modulus and their accuracies have been compared to each other. The proposed model based on artificial neural networks helps designers and technicians to estimate the resilient modulus of asphalt concretes containing RAP materials with an appropriate accuracy.

Table 1. Application of ANN in prediction of resilient modulus

Material	Inputs	Method	References
Emulsified asphalt mixtures	Curing time Cement content Residual content	Back propagation NN	[9]
Rubberized mixtures containing RAP	Rubber content RAP content Binder rheology	ANN and regression models	[10]
Fiber-reinforced asphalt concrete	Fiber content Fiber length Fiber type	Hybrid ANN-genetic algorithm model	[11]
Asphalt treated permeable base	Asphalt contents Aggregate gradations	Support vector machines and ANN	[12]

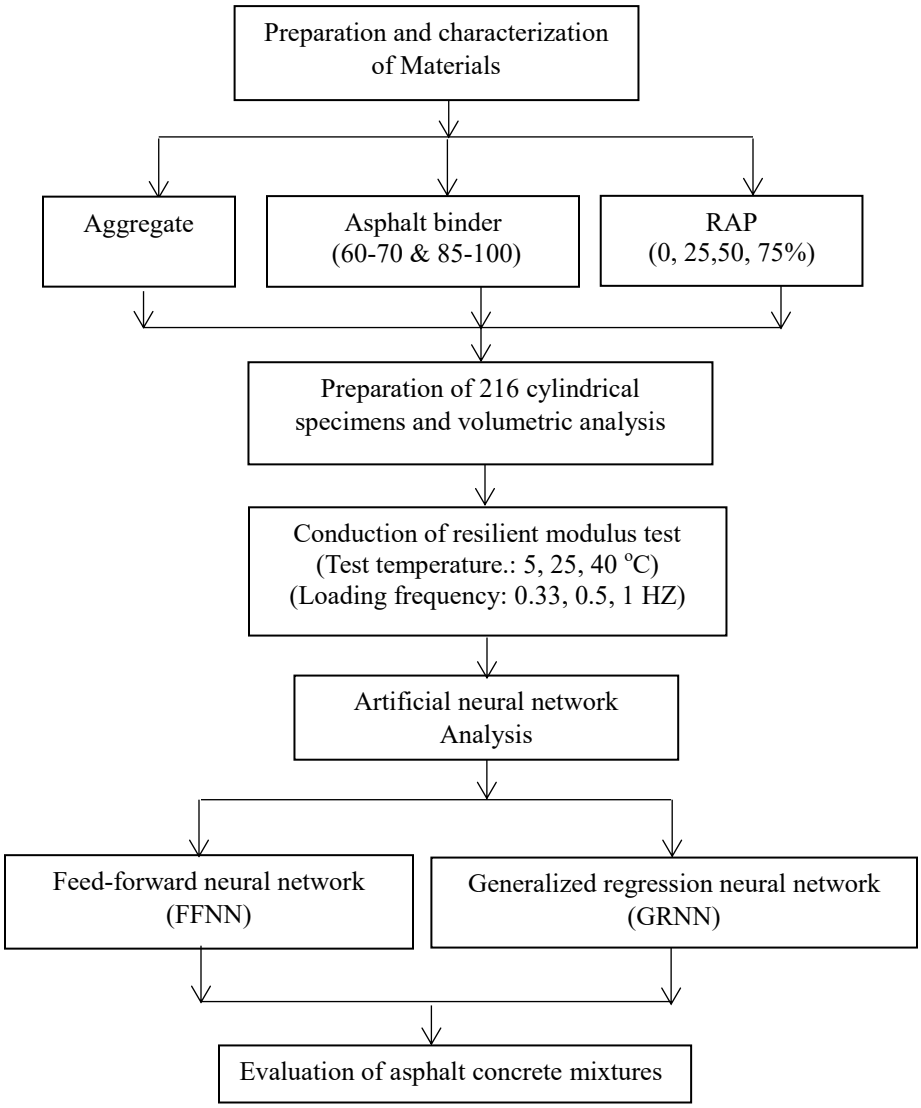

Fig. 1. Research framework.

2. Materials and Methods

2.1. Aggregate

Tables 2 and 3 show the properties and gradation of aggregates, respectively.

Table 2. Aggregate properties

Test	Result
Specific gravity	2.485
Los Angeles abrasion (%)	16
Water absorption of Fine aggregate (%)	2.5
Water absorption of Coarse aggregate) (%)	2.6
Percent fracture (two faces) (%)	81
Percent fracture (one face) (%)	93
Flakiness index	25
Elongation index	15

Table 3. Aggregate gradation

Sieve size (mm)	Passing (%)
25	100
19	92
9.5	70
4.75	50
2.36	36
0.3	11
0.075	5

2.2 Asphalt Binders

The asphalt binders used in this study were of penetration 60/70 and 85/100. Table 4 show the properties of the asphalt binders.

2.3 Reclaimed Asphalt

Tables 5 and 6 show the properties and gradation of RAP aggregates, respectively. Table 7 shows the properties of asphalt binder extracted from reclaimed asphalt.

Table 4. Properties of asphalt binders.

Test	result	
	60-70	85-100
Penetration (25° C)(0.1 mm)	69	85
Specific gravity (25° C)	1.016	1.000
Ductility (25° C) (cm)	>100	>100
Flash point (Cleveland)(°C)	310	298
Softening point (°C)	49	48
viscosity @ 120 ° C (Centistokes)	832	797
viscosity @ 135 ° C (Centistokes)	440	372
viscosity @ 150 ° C (Centistokes)	137	133

Table 5. Properties of RAP aggregate.

Test	Result
Asphalt binder content (%)	5.4
Water absorption of coarse aggregate (%)	2.1
Water absorption of fine aggregate (%)	2.51
Specific gravity of coarse aggregate	2.495
Specific gravity of fine aggregate	2.502

Table 6. Aggregate gradation of reclaimed asphalt.

Sieve size (mm)	Passing (%)
19	100
9.5	98
4.75	78
2.36	52
0.3	17
0.075	9

Table 7. Properties of extracted asphalt binder

Test	result
Softening point (°C)	72
Penetration (25° C)(0.1 mm)	20
viscosity @ 135 ° C (Centistokes)	1977

2.4. Mix Design and Specimen Preparation

In this research, Marshall mix design method (ASTM D1559) was used to determine the optimum asphalt binder contents of the control mixtures. The optimum asphalt binder contents were obtained 5.5% and 4.9% for asphalt containing asphalt binders of 60/70 and 85/100, respectively. In order to prevent the effect of asphalt binder percentage on the test results, all asphalt mixtures containing different percentages of RAP (25, 50 and 75 wt.% of the total mix) were made with the same optimum asphalt binder percentage.

2.5 Resilient Modulus Test

When a material is subjected to a stress, the induced strain will depend on the properties of the material. In general, the total strain may be divided to recoverable and non-recoverable strains. The Resilient Modulus (M_R) is defined as the ratio of applied deviator stress to the recoverable strain (Eq.1) [13].

$$M_R = \frac{\sigma_d}{\varepsilon_r} \quad (1)$$

Where ε_r is resilient or recoverable strain and σ_d is the deviator stress.

There are several methods for determining the resilient modulus of asphalt concrete mixtures. In this research study the resilient modulus test was carried out in the indirect tensile mode and in accordance with ASTM D4123 [14]. Figure 2 shows the machine used for determining the resilient modulus of the asphalt mixtures. The loading waveform was haversine. In addition the loading frequencies were 0.33, 0.5 and 1 Hz. The test was conducted at 5, 25 and 40°C and then resilient modulus (M_R) was computed using the Eq. 2. The specimens remained in the controlled-temperature chamber at each temperature for about 24 h prior to testing. Each specimen was precondition by applying 100 repeated haversine waveform load to obtain uniform deformation readout. In according to ASTM D4123 a minimum of 50 to 200 load repetitions is typical. The magnitudes of loads were 1000 N for tests at 5°C and 500 N for tests at 25°C and 40°C. In accordance with ASTM D4123 the load range should be that to induce 10 to 50% of the tensile strength.

$$M_R = \frac{P(\nu + 0.27)}{t\Delta H} \quad (2)$$

Where M_R is the resilient modulus (MPa), ν is the Poisson ratio, P is the magnitude of the dynamic load (N), ΔH is the total recoverable horizontal deformation (mm) and t is the specimen thickness (mm). The height (thickness) and diameter of the specimens were about 70 mm and 102 mm, respectively. The Poisson ratio (ν) may be computed from Eq. 3 [15].

$$\nu = 0.15 + \frac{0.35}{1+e^{(3.1849-0.04233t)}} \quad (3)$$

Where e is the base of the natural logarithm (2.7183) and t is the test temperature and is expressed in degrees Fahrenheit.

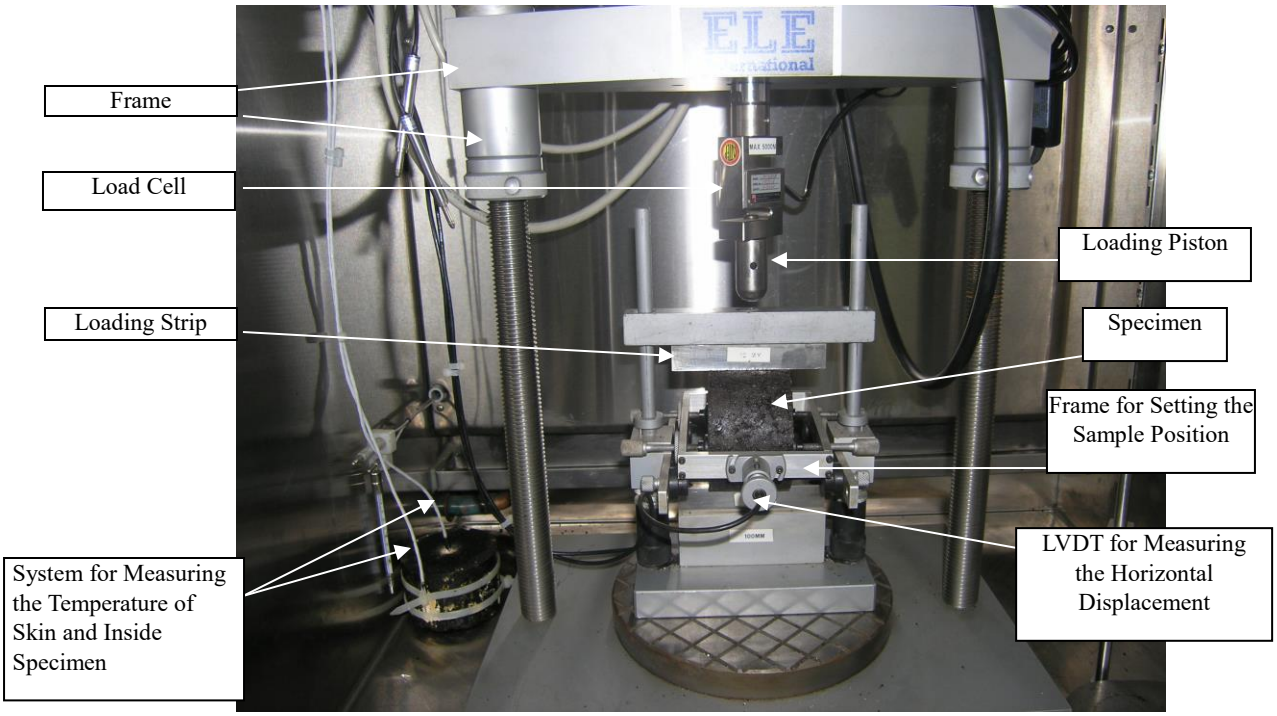

Fig. 2. Measuring the resilient modulus of asphalt concrete mixture

3. Establishment of Dataset

The final dataset was established based on the results of 214 experimental resilient modulus tests. Input variables (or predictors) were considered as temperature (5, 25, and 40 ^{o}C), penetration grade of asphalt binder (60/70 and 85/100), loading frequency (0.33, 0.5, and 1 Hz), change of asphalt binder content compared to the optimum asphalt binder content (-1, 0, and 1%), and percentage of RAP (0, 25, 50, and 75%). Output (or dependent variable) was assumed as resilient modulus of asphalt concrete mixtures in MPa. Statistical properties of different fields of experimental dataset are given in Table 8.

Table 8. Statistical properties of different fields of dataset.

Statistical Parameter	Temperature (^{o}C)	PGC[a]	Frequency (Hz)	CBC[b] (%)	RAP (%)	M_R (MPa)
Minimum	5	0	0.33	-1	0	539
Maximum	40	1	1	1	75	20883
Mean	23.18	0.50	0.61	0.00	37.85	7836.71
Standard Deviation	14.35	0.50	0.29	0.82	27.91	6074.23

[a]PGC: Penetration grade code (0 for 60/70 asphalt binder and 1 for 85/100 asphalt binder)
[b]CBC: change of asphalt binder content compared to optimum asphalt binder content

4. Modeling Using Artificial Neural Network (ANN)

According to neural networks mathematical theory, a feed-forward neural networks (FFNN) with only one hidden layer can approximate any continuous function [16]. Therefore, in recent study two types of ANN models including feed-forward neural network and general regression neural network were employed for modeling resilient modulus of asphalt concrete mixtures containing RAP with respect to different mix parameters, loading time and temperature.

In order to modeling resilient modulus, two famous architectures including (FFNN) and generalized regression neural networks (GRNN) were employed. These two architectures of neural network will be described in the next sections.

FFNN is one of the simplest type of artificial neural network type. In FFNN, the information only transmitted in one way from the input layer into the hidden layers and to the output layer [17].

Similar to the human brain, a FFNN utilizes numerous basic computational components, named artificial neurons, connected by variant weights [18]. Components of an artificial neuron is demonstrated in Figure 3. A FFNN can be trained by tuning the values of the connection weights between different neurons and after that it is able to predict a particular function. ANNs are trained so that a specific input results in a specific output. The connection weights of ANN are adjusted according to comparison of the output values and the target values until the network output values coincide the target values. Generally many such input and target value pairs are needed for network training.

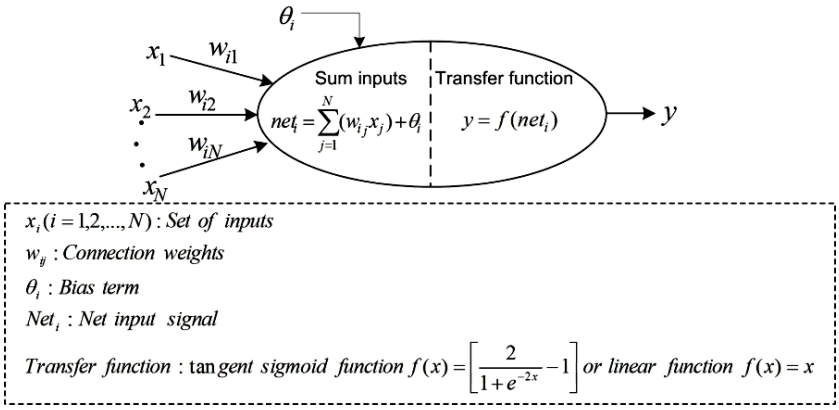

Fig. 3. A typical artificial neuron [25].

4.1. Feed-Forward Neural Network (FFNN)

The back propagation algorithm is commonly used for training of a FFNN which involves two stages [19, 20]:

Forward stage. In this stage, the network's free parameters are set and the input signal from the input layer is transmitted to the hidden layer and then into the output layer. The forward stage finishes with an error signal calculation.

$$e_i = d_i - y_i \quad (4)$$

where d_i denotes the target response, and y_i denotes the predicted output by the ANN resulted from input x_i.

Backward stage. During this stage, the error signal e is transmitted through the ANN in

the backward or reverse direction. In point of fact, tuning of network's free parameters are implemented in this stage in order to minimize the error e in a statistical context.
In this research, the back propagation training algorithm of Levenberg - Marquardt was employed. The architecture of a FFBP has been presented in Figure 4.

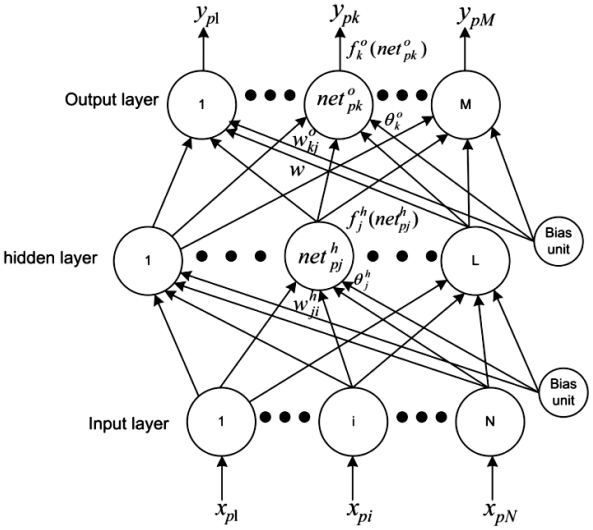

Fig. 4. A three layer feed-forward backpropagation network architecture [21].

4.2. General Regression Neural Network (GRNN)

Specht was the first one who proposed the Generalized Regression Neural Network (GRNN) [22].
GRNN is a version of ANNs that utilizes brain synapse-like framework for handling data. The GRNN has excellent approximation capability and learning speed, specifically for large sample datasets. The GRNN also has excellent forecast results, in case of relatively small datasets[23].
GRNN aims to predict the output vector $Y=[y_1,y_2,\ldots,y_k]^T$ based on the input vector $X=[x_1, x_2,\ldots,x_n]^T$ by means of a linear or nonlinear regression surface. The GRNN model can be write as follows:

$$E[Y \mid X] = \frac{\int_{-\infty}^{\infty} Yf(Y,X)dX}{\int_{-\infty}^{\infty} f(Y,X)dX} \quad (5)$$

where X denotes the input vector with dimension of n, Y is the estimated output value by GRNN model, E[Y|X] is the target value of the output Y, given the input vector X and f(Y,X) is the joint probability density function of X and Y.
GRNN is arranged using four layers including layer of input, layer of pattern, layer of summation and layer of output (Figure 5). The layer of input receives and saves input parameters to an input vector X. The number of neurons in the input layer is similar to the input vector dimension. Then, the data are transmitted from input layer are fed to the pattern layer.
The pattern layer performs a non-linear mapping from the input space to the pattern space. The neurons in the pattern layer can memorize the relationship between the input neuron and the proper response of pattern layer. The number of neurons in the pattern layer is the same as the number of input variables. The pattern Gaussian function of p_i can be expressed as:

$$p_i = \exp\left[-\frac{(X-X_i)^T(X-X_i)}{2\sigma^2}\right] \quad (i=1,2,...,n) \quad (6)$$

Where σ denotes the smoothing parameter, X denotes the input variable and X_i is a specific training vector of the neuron i in the pattern layer.
The summation layer consists of two summations including simple summation (S_s) and weighted summation (S_w). S_s and S_w calculate the arithmetic sum of the pattern layer outputs and the weighted sum of the pattern layer outputs, respectively (Eqs. 7 and 8).

$$S_s = \sum_{i=1} p_i \quad (7)$$

$$S_w = \sum_{i=1} w_i p_i \quad (8)$$

Where w_i is the weight of connection between pattern neuron i and summation layer.

The number of neurons in the output layer is equal to the dimension k of the output vector Y. After commutating the summations of neurons in the summation layer, they are fed into the output layer. The output Y of the GRNN model can be determined as follows:

$$Y = \frac{S_s}{S_w} \quad (9)$$

It is evident that the GRNN model has only one parameter σ which needs to be tuned. This parameter sets the generalization capability of the GRNN.

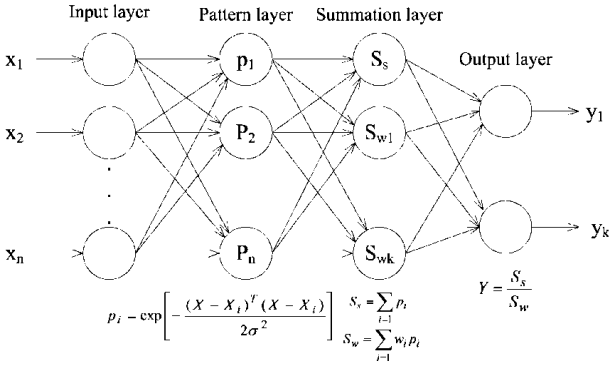

Fig. 5. Architecture of GRNN [24].

4.3. Evaluation of Models Performance

In the present study, the performances of FFNN and GRNN were evaluated according to the following statistical indicators (Eqs. 10 and 11):

Root Mean Square Error (RMSE):

$$RMSE = \sqrt{\frac{1}{N}\sum_{i=1}^{N}(y_i - x_i)^2} \quad (10)$$

Coefficient of determination (R^2):

$$R^2 = \left[\frac{1}{N}\frac{\sum_{i=1}^{N}(x_i - \bar{x})(y_i - \bar{y})}{\sigma_x.\sigma_y}\right]^2 \quad (11)$$

where N denotes the size of observations vector, x_i denotes the x value for observation i, y_i denotes the y value for prediction i, $\bar{x}$ denotes the mean x value, $\bar{y}$ denotes the mean y value, σ_x denotes the standard deviation of x, and σ_y denotes the standard deviation of y.

5. Optimum Architecture and Performance of ANN Models

5.1. Optimum Architecture of FFNN

The FFNN performance greatly depends on the ANN architecture and setting of parameters. An important task in developing a FFNN is finding the optimum number of hidden layers as well as optimum number of neurons in each hidden layer. This task is commonly completed by trial and error approach. On the other hand, the setting of original weight and bias values has a major impact on the results of the FFNN.

In this study, the ANN toolbox of Matlab was employed for implementation of FFNN. Matlab ANN toolbox automatically selects the initial values for weights and biases for each run, which affects the performance of the trained ANN considerably, even if all parameters and ANN architecture remain constant. This leads to additional difficulties in choosing the optimum network architecture and initial value of parameters. To overcome this difficulty, a code was developed in Matlab which handles the trial and error process, automatically. This code checks various numbers of the neurons in the hidden layer for several times and chooses the best ANN architecture based on the minimum RMSE (Root Mean Squared Error) for overall dataset. The testing (20%), cross validating (10%) and training (70%) sets for

ANN training procedure were selected randomly from the established dataset. The optimal structure of ANN was determined as 5-14-1 (one hidden layer with 14 neurons). The transfer function for hidden and output layer was assumed as hyperbolic tangent sigmoid and linear transfer functions, respectively. Weights and bias matrix are presented in appendix A.

5.2. Optimum Architecture of GRNN

Matlab ANN toolbox was employed in this research study for training and testing of GRNN model. The smoothing parameter of σ affects the generalization capability of the GRNN and should be set to an appropriate value for optimal performance of GRNN. In order to determine the optimum value of smoothing parameter, a program was developed in Matlab. This program was able to train GRNN according to different values of spread parameter. In case of each value of smoothing parameter (σ could varies from 0.001 to 1 with increment of 0.001), the value of RMSE for testing set was determined and the value that results in minimum value of RMSE was selected as optimum value of smoothing parameter. 80% of dataset records were selected as training set and remaining 20% were considered as testing set. Training set in case of GRNN was the union of training and cross validation sets of FFNN and testing set was the same for both neural network models. Variation of RMSE versus spread parameters for both training and testing sets is demonstrated in Figure 6. According to the Figure 6, by increasing the smoothing parameter, the RMSE of training set increases, but the minimum RMSE of testing set is achieved when the value of smoothing parameters is equal to 0.157.

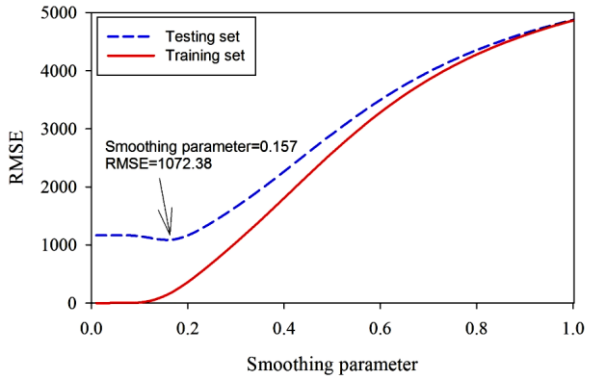

Fig. 6. RMSE versus smoothing parameter.

5.3. Performances of FFNN and GRNN

The performances of FFNN and GRNN for predicting resilient modulus using training and testing sets are demonstrated in Figures 7 to 10. Also, the RMSE and R^2 values for each model are given in Table 9.

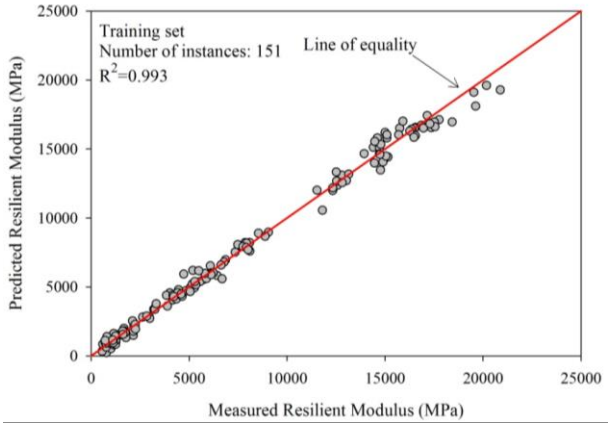

Fig. 7. Performance of FFNN model (training set).

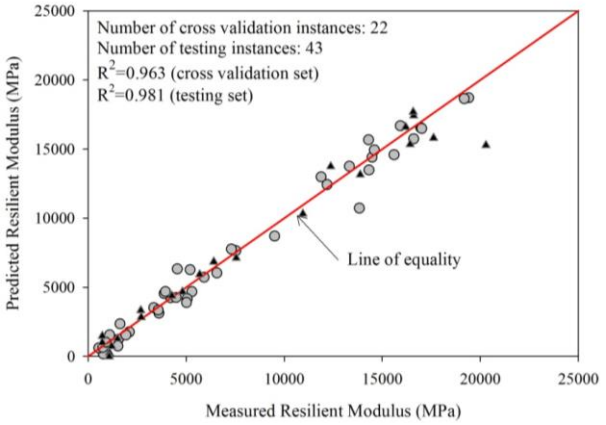

Fig. 8. Performance of FFNN model (testing set).

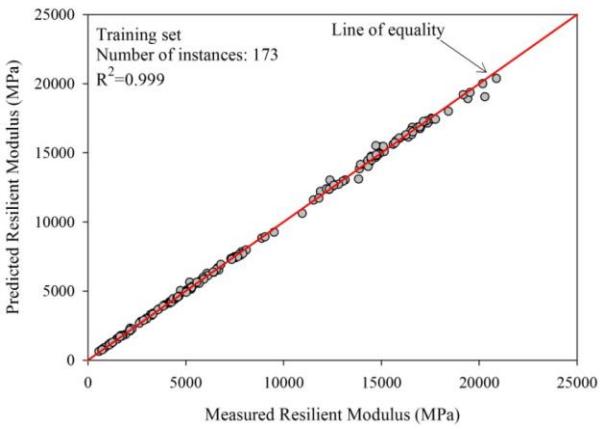

Fig. 9. Performance of GRNN model (training set).

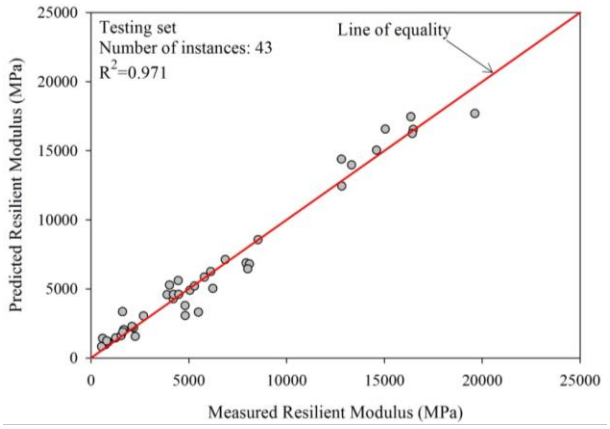

Fig. 10. Performance of GRNN model (testing set).

Table 9. The accuracy of different artificial neural network models

Model	Training Set		Testing Set	
	R^2	RMSE	R^2	RMSE
FFNN	0.993	502.95	0.981	827.20
GRNN	0.999	142.33	0.971	1017.46

According to Table 9, in case of FFNN, the coefficient of determination (R^2) between observed and predicted values of resilient modulus for training and testing sets is 0.993 and 0.981, respectively. These two values are 0.999 and 0.971 for GRNN. It is evidence that the accuracy of FFNN model is superior to GRNN. In this case, the FFNN model is capable to predict resilient modulus of asphalt concrete with R^2 more than 0.98.

6. Parametric Analysis

In order to investigate the effect of various factors such as the temperature, penetration grade of asphalt binder, loading frequency, change of asphalt binder content compared to optimum asphalt binder content, and percentage of RAP on the resilient modulus of asphalt concrete mixtures, one asphalt concrete mixture under standard conditions was assumed. The assumed asphalt concrete mixture with standard conditions is given in Table 10.

Table 10. Standard conditions for parametric analysis.

Temp.(°C)	PGC[a]	Frequency (Hz)	CBC[b] (%)	RAP (%)
25	0	0.5	0	25

[a]PGC: Penetration grade code (0 for 60/70 asphalt binder and 1 for 85/100 asphalt binder)
[b]CBC: change of asphalt binder content compared to optimum asphalt binder content

To study the effect of different parameters, on the resilient modulus, the trained FFNN was used and by changing the desired parameters, the resilient modulus was computed. The results of the parametric analysis are presented in Figures 11 to 15.

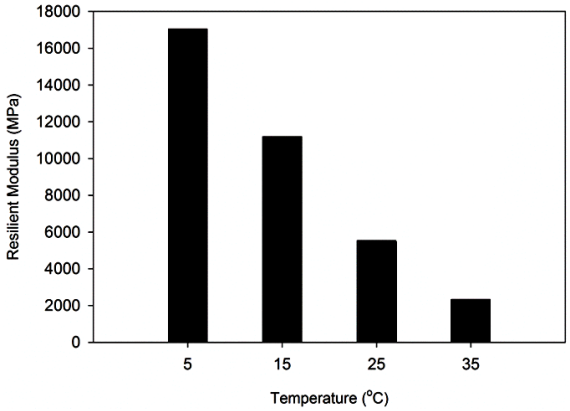

Fig. 11. Resilient modulus versus temperatures for the asphalt mixture.

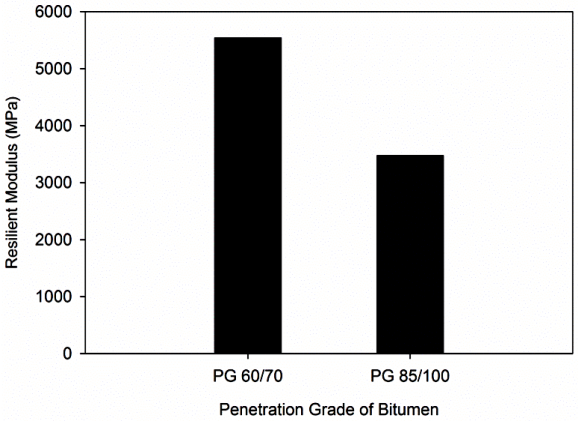

Fig. 12. Effect of penetration grade of asphalt binder on the resilient modulus of asphalt concrete mixture.

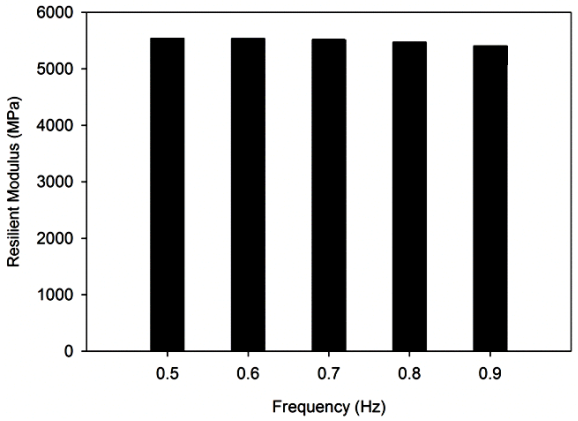

Fig. 13. Effect of loading frequency on the resilient modulus of asphalt mixure.

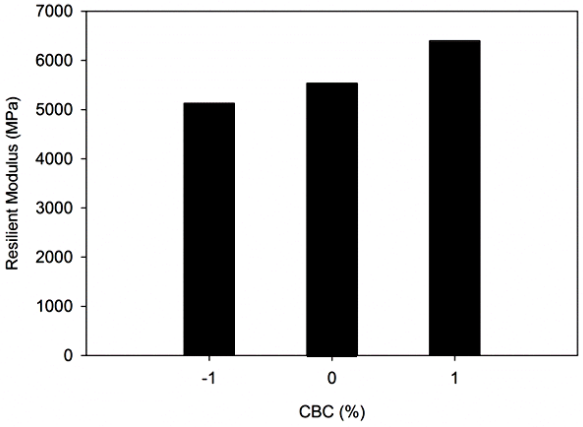

Fig. 14. Effect of CBC parameter on the resilient modulus of asphalt mixure.

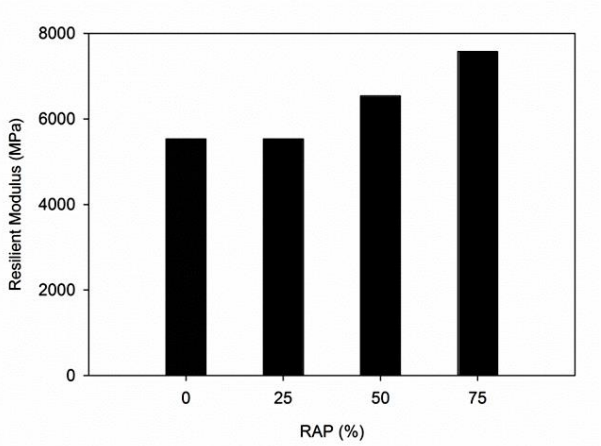

Fig. 15. Effect of RAP content on the resilient modulus of asphalt concrete mixture

According to Figures 11 to 15, the effect of different parameters on the resilient modulus of asphalt concrete mixtures can be stated as follows:

Temperature: by increasing the temperature, the resilient modulus of asphalt mixes decreases and vice versa. Due to visoelastic behavior of asphalt materials, by increasing temperature, the viscosity of asphalt binder decreases and thus the stiffness of asphalt concrete decreases.

Change of asphalt binder content compared to optimum asphalt binder content: by increasing asphalt binder content compared to optimum asphalt binder content, resilient modulus increases. Also by decreasing asphalt binder content compared to optimum asphalt binder content, resilient modulus decreases. As the asphalt binder content increases, the adhesion and tensile strength in the mixture structure improves. This leads to decrease in the horizontal deformation in the resilient modulus test, so in according to equation 2, the resilient modulus of asphalt concrete mixtures increases. However it should be noted that if the asphalt binder content increases so much, the excess asphalt binder will weak the interlocking the

aggregate and so the resilient modulus of asphalt concrete mixture will decrease.

Penetration grade of asphalt binder: by increasing the Penetration grade, the resilient modulus of asphalt mixes decreases and vice versa. Asphalt binder with higher penetration grade has lower viscosity and this decreases the stiffness and resilient modulus of the asphalt concrete mixtures.

Loading frequency: by changing loading frequency between 0.5 to 0.9 Hz, no distinctive change is observed for resilient modulus. This can be explained by narrow range of frequency change.

In fact for exploring the effect of frequency on the resilient modulus of asphalt concrete, the frequency should be changed in a wide range specially for moderate and low temperatures.For further research, it is recommended that a wide range of frequencies (from 0.1 to 10) to be used for experimental program.

RAP content: By Increasing RAP content, the resilient modulus of asphalt mixes increases, significantly. Since, RAP contains aged asphalt binder, so the addition of RAP makes the mixture stiffer and increases the resilient modulus. It should be noted that although the increasing of resilient modulus may considered as a positive parameter for pavement design, but the other properties such as fatigue and rutting resistance of asphalt concrete mixture containing RAP should be evaluated.

7. Conclusion

In this study, two different versions of artificial neural networks including FFNN and GRNN, were employed for modeling of the resilient modulus of asphalt concrete mixtures containing reclaimed asphalt pavement. In ANN architecture, temperature (^{o}C), penetration grade code (0 for 60/70 asphalt binder and 1 for 85/100 asphalt binder), loading frequency (Hz), change of asphalt binder content compared to optimum asphalt binder content (%), and RAP content (%) were chosen as the input parameters and the resilient modulus (MPa) of asphalt concrete mixtures was assumed as the output parameter.

According to the results of this study the following statements can be concluded:

- The optimum architecture of FFNN for predicting resilient modulus was determined as 5-14-1 (one hidden layer) with hyperbolic tangent sigmoid and linear transfer functions for the hidden layer and output layer, respectively. R^2 and RMSE for predicted values of resilient modulus using FFNN was determined as 0.981 and 827.20 for testing set, while these values are 0.971 and 1017.46 in case of GRNN. Thus, the accuracy of FFNN model was superior to GRNN model for predicting resilient modulus of asphalt concrete mixtures containing RAP materials.
- The most effective parameter on the resilient modulus of asphalt concrete mixtures containing RAP materials was temperature.
- The resilient modulus of asphalt concrete mixtures increased when the RAP content increases or stiffer asphalt binder is employed.
- Results of this study also showed that by decreasing temperature and increasing asphalt binder content compared to optimum asphalt binder content, resilient modulus increases.

REFERENCES

[1] West, R.C., Rada, G.R., Willis, J.R., Marasteanu, M.O. (2013), NCHRP report 752, Improved Mix Design, Evaluation and Materials Management Practices for

Hot Mix Asphalt with High Reclaimed Asphalt Pavement Content, TRB, National Research Council, Washington, DC, USA.

[2] Colbert, B., You, Z. (2012). The Determination of Mechanical Performance of Laboratory Produced Hot Mix Asphalt Mixtures Using Controlled RAP and Virgin Aggregate Size Fractions, Construction and Building Materials, 26:655-662. (DOI: 10.1016/j.conbuildmat.2011.06.068)

[3] Sondag, M.S., Chadbourn, B.A., Drescher, A. (2002). Investigation of Recycled Asphalt Pavement (RAP) Mixtures, Minnesota Department of Transportation, Report No: MN/RC - 2002-15.

[4] Zaumanis, M., Mallick, R.B. (2015). Review of Very High-Content Reclaimed Asphalt Use in Plant-Produced Pavements: State of the Art, International Journal of Pavement Engineering, 16: 39-55. (DOI: 10.1080/10298436.2014.893331)

[5] Tarefder, R.A., White, L., Zaman, M. (2005). Neural Network Model for Asphalt Concrete Permeability, Journal of Materials in Civil Engineering, 17:19-27. (DOI: 10.1061/(ASCE)0899-1561(2005)17:1(19))

[6] Ozgan, E. (2011). Artificial Neural Network Based Modeling of the Marshall Stability of Asphalt Concrete, Expert Systems with Applications, 38:6025-6030. (DOI: 10.1016/j.eswa.2010.11.018)

[7] Xiao, F., Amirkhanian, S.N. (2009). Artificial Neural Network Approach to Estimating Stiffness Behavior of Rubberized Asphalt Concrete Containing Reclaimed Asphalt Pavement, Journal of Transportation Engineering, 135:580-589. (DOI: 10.1061/(ASCE)TE.1943-5436.0000014)

[8] Zeghal, M. (2008). Modeling the Creep Compliance of Asphalt Concrete Using the Artificial Neural Network Technique, GeoCongress: Characterization, Monitoring and Modeling of GeoSystems, 910-916. (DOI: 10.1061/40972(311)114)

[9] Ozsahin, T.S., Oruc, S. (2008). Neural Network Model for Resilient Modulus of Emulsified Asphalt Mixtures, Construction and Building Materials, **22**:1436-1445. (DOI:10.1016/j.conbuildmat.2007.01.031)

[10] Xiao, F., Amirkhanian, S.N. (2008). Effects of Binders on Resilient Modulus of Rubberized Mixtures Containing RAP Using Artificial Neural Network Approach, Journal of Testing and Evaluation, **37**:129-138. (DOI: 10.1520/JTE101834)

[11] Vadood, M., Johari, M.S., and Rahai, A. (2015). Developing a Hybrid Artificial Neural Network-Genetic Algorithm Model to Predict Resilient Modulus of Polypropylene/Polyester Fiber-Reinforced Asphalt Concrete, The Journal of the Textile Institute, 106:1239-1250. (DOI: 10.1080/00405000.2014.985882)

[12] Kezhen, Y., Yin, H., Liao, H., Huang, L. (2011) Prediction of Resilient Modulus of Asphalt Pavement Material Using Support Vector Machine, Road pavement and material characterization, modeling, and maintenance, 16-23. (DOI: 10.1061/47624(403)3)

[13] Huang, Y.H. (2004), Pavement Design and Analysis. Pearson/Prentice Hall.

[14] ASTM D4123, Standard Test Method for Indirect Tension Test for Resilient Modulus of Bituminous Mixtures. (1995) West Conshohocken, PA: ASTM International, USA.

[15] Witzcak, M.W., Kaloush, K., Pellinen, T., El-Basyouny, M, Von Quintus, H. (2002). Simple Performance Test for Superpave Mix Design (Vol. 465), TRB, National Research Council, Washington, DC, USA.

[16] Hornik, K. (1991). Approximation Capabilities of Multilayer Feed-forward Networks, Neural Networks, 4:251–257. (DOI: 10.1016/0893-6080(91)90009-T)

[17] Hagan, M.T., Demuth, H.B., Beale M.H. (1996), Neural Network Design, PWS Pub. Co., Boston, USA.

[18] Haykin, S.S. (2001), Neural Networks: a Comprehensive Foundation, Tsinghua University Press.

[19] Werbos, P. (1974), Beyond regression: New Tools for Prediction and Analysis in the Behavioral Sciences.

[20] Rumelhart, D.E., Hinton G.E., Williams, R.J. (1988). Learning Representations by back-Propagating Errors, Cognitive Modeling 5:1.

[21] Freeman, J.A., Skapura, D.M., (1992), Neural Networks: Algorithms, Applications and Programming Techniques, Addison-Wesley Publishing Company.

[22] Specht, D.F., (1991). A General Regression Neural Network, IEEE Transactions on Neural Networks, 2:568-576. (DOI: 10.1109/72.97934)

[23] Li, H.Z., Guo, S., Li, C.J., Sun, J.Q. (2013). A Hybrid Annual Power Load Forecasting Model Based on Generalized Regression Neural Network with Fruit Fly Optimization Algorithm, Knowledge-Based Systems, 37:378-387. (DOI: 10.1016/j.knosys.2012.08.015)

[24] Leung, M.T., Chen, A.S., Daouk, H. (2002). Forecasting Exchange Rates Using General Regression Neural Networks, Computers & Operations Research, (DOI: 27:1093–1110. 10.1016/S0305-0548(99)00144-6)

Appendix A. Weights and biases of Artificial Neural Network (ANN)

This Appendix is assigned to input vector, output vector, weight factors, and bias factors of the back propagation neural network which was discussed in section 4.5. The optimum architecture of back propagation neural network is 5-14-1 with sigmoid transfer function in the hidden layer and linear transfer function in the output layer. The order of normalized predictors in the input vector is as follows:

$$\mathrm{I}=\left\{\mathrm{T,PGC,Frequency,CBC,RAP}\right\}_{1\times5} \quad (12)$$

The order of normalized output parameters in the output vector is as follows:

$$\mathrm{O}=\left\{\mathrm{Mr}\right\}_{1\times1} \quad (13)$$

Equation (14) may be used for simulation of ANN and prediction of resilient modulus based on given input vector.

$$\{\mathrm{Out}\}=\mathrm{tansig}\left(\{\mathrm{Inp}\}\times[\mathrm{W_h}]^{\mathrm{T}}+\{\theta_{\mathrm{h}}\}^{\mathrm{T}}\right)\times[\mathrm{W_o}]^{\mathrm{T}}+\{\theta_{\mathrm{o}}\}^{\mathrm{T}} \quad (14)$$

Where tansig (x) can be obtained as follows:

$$\mathrm{tansig(x)}=\frac{2}{1+\mathrm{e}^{-2\mathrm{x}}}-1 \quad (15)$$

Weight matrix for hidden and output layers are given in Table 11 and Table 12, respectively. Bias vector for hidden and output layer are given in Table 13 and Table 14, respectively.

Table 11. Weight matrix of hidden layer $(W^h)^{\mathrm{t}}{}_{14\times5}$

-0.299643482	0.331131154	-0.150468515	3.894341144	-1.668650763
1.245192212	-0.474771598	-0.018442791	-2.452333208	3.068082506
1.748791212	0.145061223	-0.767821500	0.608096855	-0.051696506
-1.423850700	0.280712802	-0.191103718	0.395230798	-0.118328016
-1.809273169	0.145292928	1.949744431	0.989839148	-2.461689208
-0.922523725	0.689167058	0.620551910	-1.382514250	1.110017441
2.213075920	1.798941169	1.390372619	0.573364045	-0.215540190
-2.105617879	0.003661187	0.046071359	-0.625417854	0.838355064
-1.101012107	-1.135496135	0.468455867	-7.184626798	-0.977689316
2.425698003	1.168375909	-0.318634537	-1.986476824	-0.819925948
2.054786137	-1.787104430	0.994535680	2.862659074	-2.284213323
0.960594508	-0.912956687	-0.138879608	3.623386289	2.789123777
-0.290257636	1.097970413	0.150710357	-1.003233075	2.653275383
-0.762431346	-1.915528492	1.229452135	1.775558134	1.225965169

Table 12. Weight matrix of output layer (W^o)

14×1
-0.295478876
-0.204809027
0.083193339
0.397573892
0.024329070
0.064349455
-0.060940316
0.289739736
0.077479325
-0.104030104
0.057266017
0.105736230
0.175164928
0.022502847

Bias vector for hidden and output layer are given in Table 13 and Table 14, respectively:

Table 13. Bias vector of hidden layer (θ^h)

-4.765303345
3.153745569
-2.332963106
-0.607005988
-1.178814078
1.336729674
1.370637157
0.275829938
-2.188464110
1.655692989
-1.621861283
2.530472150
-4.183043913
-2.608443726

Table 14. Bias vector of output layer (θ^o)

-0.017525849